Ученые записки Таврического национального университета им. В. И. Вернадского
Серия «Биология, химия». Том 24 (63). 2011. № 3. С. 48-56.

UDC 548.32

STUDY THE CRYSTAL STRUCTURE OF THE COMPOSITION $Pb_{8-x}Eu_xNa_2(PO_4)_6\square_{2-x/2}O_{x/2}$

Getman E.I., Ignatov A.V., Mohammed A.B. Abdul jabar, Loboda S.N.

Donetsk National University, Donetsk, Ukraine
E-mail: mohammed_samraey@yahoo.com

The substitution of europium by lead in the compound $Pb_8Na_2(PO_4)_6\square_2$, in accordance with the scheme $Pb^{2+} + ½\square \rightarrow Eu^{3+} + ½O^{2-}$ has been investigated by infrared spectroscopy, scanning electron microscopy and powder X-ray diffraction methods, that corresponds to the compound of solid solutions $Pb_{(8-x)}Eu_xNa_2(PO_4)_6\square_{(2-x/2)}O_{(x/2)}$ ($0 \le x \le 2{,}0$). It was established that single-phase solid solutions, synthesized by solid state reaction at 800ºC, are formed in the range from x=0.0 up to x=1.0. Refinement of the crystal structure of some samples was performed using the Rietveld method. Established that europium ions are located in positions Pb(2), resulting in the distance in a polyhedron Pb(2) the structure of apatite decreased.
Keywords: apatite structure, solid solution, lead, europium.

INTRODUCTION

Apatites are generally described in the hexagonal symmetry group $P6_3/m$ and have the general composition $M_{10}(EO_4)_6(Z)_2$, where M- one, two and trivalent cations (Na^+, K^+, Ca^{2+}, Sr^{2+}, Ba^{2+}, Pb^{2+}, Cd^{2+}, Eu^{3+}, Y^{3+}, La^{3+}, ions lanthanide etc.), E - four-, five- and hexavalent cations (Si^{4+}, Ge^{4+}, P^{5+}, V^{5+}, As^{5+}, S^{6+}, Cr^{6+}, etc.), Z - anions OH^-, F^-, Cl^-, Br^-, I^-, O^{2-} and vacancy ($\square$).

The structure of apatite is characterized by the presence of two structurally nonequivalent positions in the cation sublattice conventionally designated M(1) and M(2). Position M(1) has a circle of nine oxygen atoms (each of which is part of the PO_4 tetrahedral), forming a coordination polyhedron – nine vertex polyhedron. Coordination environment positions M(2) consists of six oxygen atoms belonging to the PO_4 tetrahedral, and F^-(Cl^-, OH^-, O^{2-}, etc.) ions, which form the coordination polyhedron – seven vertex polyhedron. Equilateral triangles M(2) in the apatite structure form a channel, which are F^-(Cl^-, OH^-, O^{2-}, etc.) ions.

In recent years, the interest of researchers toward compounds with this structure does not weaken, at least for two reasons. First, they possess a practically important property and can be used, for example, as solid stable forms for disposal of radioactive waste, sorbents [1, 2, p. 10], as solid electrolytes [3, p. 10], catalysts [4, p. 10], phosphors, laser materials [5, p. 10], and in many other cases. Secondly, they characterized by a wide range of isomorphism substitutions, allowing isomorphic components by introducing adjust their properties. In particular, by partial substitution in the apatite structure of divalent ions of rare-earth elements on the other elements are luminescent and laser materials [6, 7, p. 10].

Therefore, relevant research heterovalent substitution scheme $M^{2+} + Z^{-} \rightarrow Ln^{3+} + O^{2-}$ in the systems $M_{(10-x)}Ln_x(EO_4)_6Z_{(2-x)}O_x$, where M^{2+} - ions of divalent elements, Ln^{3+} - ions of rare-earth elements. So far, substitution of alkaline studied in most rare earth elements (for example, [8-10, p. 10]). However, despite the fact that the ionic radius of lead is similar in size to the radii of ions of alkaline earth elements, no published information about the substitution of lead by rare earth elements in the systems $Pb_{(10-x)}Ln_x(PO_4)_6OH_{(2-x)}O_x$. Advantages systems of the lead apatites are significantly lower temperature synthesis (800˚C [11, p. 10]) compared with systems of the apatite of alkaline earth elements (1200-1450˚C [8, p. 10]), which simplifies the method of synthesis and helps to ensure a fine grain.

Thereby, it is interesting to study the substitution in following scheme: $2Pb^{2+}+\square \rightarrow 2Eu^{3+}+O^{2-}$, as described for the systems $Pb_{(8-x)}Ln_xNa_2(PO_4)_6\square_{(2-x/2)}O_{(x/2)}$ (Ln = Ce, Pr, Nd, Sm, Eu, Gd, Tb, Dy, Ho, Er). However, these systems have been studied only for compositions with x= 0.25 [12, p. 10]. In this paper we study the substitution of lead by europium in the compound $Pb_8Na_2(PO_4)_6\square_{2-x/2}$ in a wide range of compositions.

MATERIALS AND METHODS

1.1. Synthesis: As starting reagents for apatite synthesis, we used PbO (chemically pure), Eu_2O_3 (99.99%), Na_2CO_3 (chemically pure) and $(NH_4)_2HPO_4$ (analytical grade). Samples corresponding to $Pb_{(8-x)}Eu_xNa_2(PO_4)_6\square_{(2-x/2)}O_{(x/2)}$ ($0 \le x \le 2$) were synthesized by solid state reaction. One sample was prepared for each value of x in the preceding formula from 0 to 2.0 with an x increment of 0.2. All samples were synthesized according to the following reaction:

$(8-x)PbO+6(NH_4)_2HPO_4+Na_2CO_3+(x/2)Eu_2O_3 \rightarrow Pb_{(8-x)}Eu_xNa_2(PO_4)_6\square_{(2-x/2)}O_{(x/2)} + 9H_2O+ CO_2+ 12NH_3$

A mixture of initial components with a total weight of 1g was ground in a mortar, followed by successive annealing steps in alumina crucibles at 300 C for 3 h, and finally at 800°C for 72 h with intermittent grindings at the last temperature step.

The duration of annealing for the last temperature step was determined by attaining stable phase composition of synthesized samples. Reaching equilibrium and stable phase composition in $Pb_{(8-x)}Eu_xNa_2(PO_4)_6\square_{(2-x/2)}O_{(x/2)}$ apatites becomes more difficult as europium atomic number increase. The system takes several intermittent grindings to reach equilibrium at 800°C.

1.2. Characterizations: The materials synthesized were characterized by the following conventional techniques. X-ray powder diffraction (XRD) was carried out with a DRON-3 diffractometer, using monochromatic Ni-filtered Cu Kα radiation (λ=1.54178). The pattern was scanned in steps of 2θ=0.05˚, in the range 15-140˚ at a counting time 3 s for each step. The data were analyzed using the Rietveld method with the program FullProf.2k (version 3.40) [13, p. 10] and with graphic interface WinPLOTR [14, p. 10].

Transmission infrared spectra were taken by the KBr method using a Fourier transform infrared spectroremeter (FT-IR TENSOR 27 (Bruker Optics)) in the range (4000-400) cm^{-1}. The infrared absorption spectrum was carried out on a pellet sample, which prepared by crushing 1 mg samples with 600 mg KBr (samples + KBr). Estimate grain size and semi-quantitative elemental analysis was performed on a scanning electron microscopy with X-ray microanalysis in a scanning electron microscope JSM-6490L V

(JEOL, Japan) with energy dispersive spectrometer INCA Penta FETx3 (OXFORD Instruments, England). Differences in the experimental and theoretical content of the elements do not exceed 2%, which is acceptable for this method of analysis in such systems.

RESULTS AND DISCUSSION

The X-ray diffraction patterns of the samples with different value x obtained by solid state reaction are shown in Fig. 1. As seen from Fig. 1, in the composition range x = 0.0 up to 0.8 diffractogram shows only reflections of phase with the structure of apatite (reflections of pure apatite) [15, p. 10]. In samples x = 1.0 and x =1.2 in the diffractogram shown, beside reflections the structure of apatite, found a reflection whose intensity is about 3 % compared with the maximum intensity reflection structure of apatite. Since its intensity is almost independent of the value of x, we can assume that either the superstructure reflections or reflection component that is not part isomorphic to the structure. In the composition range x = 1.4 – 2.0 in X-ray diffractogram, there are also reflections of the structure of europium phosphate EuPO4, whose intensity increases with the value of x increases regularly. This suggests that the limit of the isomorphism substitution corresponds with the value x <1.0.

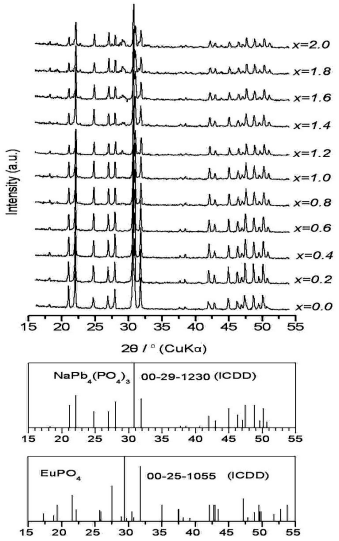

Fig. 1. The X-ray diffraction patterns of $Pb_{(8-x)}Eu_xNa_2(PO_4)_6\square_{(2-x/2)}O_{(x/2)}$, and diffractograms the phase identification of $Pb_8Na_2(PO_4)_3$ and $EuPO_4$ based on data base pdf-2 (ICDD).

A plot of parameters *a* and *c* of the $Pb_{(8-x)}Eu_xNa_2(PO_4)_6\square_{(2-x/2)}O_{(x/2)}$ hexagonal unit cell vs degree of substitution by europium (*x*) is shown in (Fig. 2). The unit cell parameters a and c do not linearly with the compositions (fig. 2). Reason that, the crystal ionic radius of ion Eu3+ (1.087 Å) smaller than ion Pb2+ (1,33 Å) at 0,21 Å (hereafter

sizes taken for coordination number 6 [16, p. 10]) causes a decrease of unit cell parameters a and c with the increase of value x from 0.0 to 2.0 (the error in determining the cell parameters is within ± 0,003 Å).

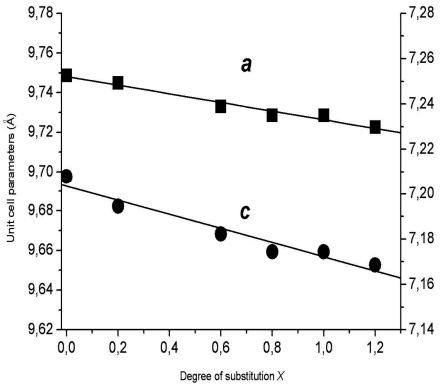

Fig. 2. Plot of hexagonal unit cell parameters *a* and *c* vs degree of Eu substitution Pb in the system $Pb_{(8-x)}Eu_xNa_2(PO_4)_6\square_{(2-x/2)}O_{(x/2)}$.

Due to a decrease of cell parameters refinement limit of substitution was also carried out by the "disappearing phase" method. We estimated the europium substitution limit in the apatite by extrapolating the linear relationship of intensity of the largest phosphate europium $EuPO_4$ peak (120) vs the degree of substitution to the intersection with the abscissa axis. Accordingly, the horizontal axis (Fig. 3) gives the limit of substitution of europium in $Pb_{(8-x)}Eu_xNa_2(PO_4)_6\square_{(2-x/2)}O_{(x/2)}$ at x =1,206, in good agreement with the value which shown in Figure 2.

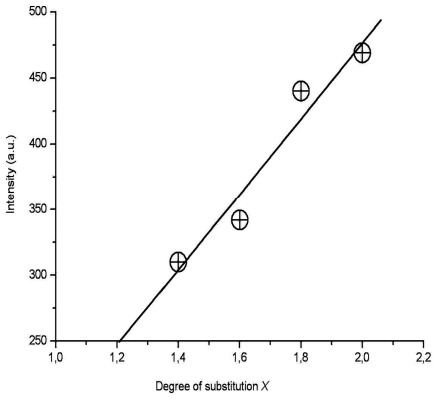

Figure 3. Plot of the intensity of (120) reflection for EuPO4 vs degree of substitution, *x*.

The samples of the composition $Pb_{(8-x)}Eu_xNa_2(PO_4)_6\square_{(2-x/2)}O_{(x/2)}$ were examination by SEM revealed particles 2.0 and 5.0 μm successively. Figs. 4(a), 4(b), 4(c) and 4(d) and present SEM images the grain sizes ranged from several dozen to several hundred nanometers. Due to the fact that lead oxide in the synthesis conditions can sublimate was conducted semi-quantitative elemental analysis for Pb, P, Eu, O and Na for samples with the values x=0.0 and 0.4, whose result are presented in Table 1. For the sample with x=0 determine the content of elements was carried out in 24 points on five sections (in brackets are calculated values). Table 1 show results of many samples, which composition by SEM (scanning electronic microscopy) analyze.

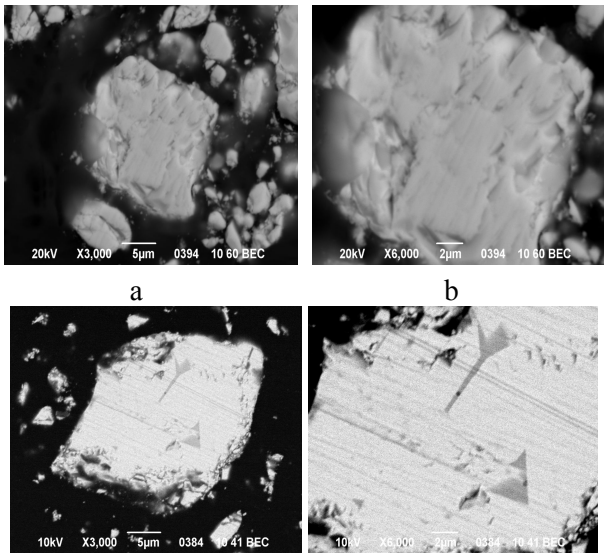

Figs. 4. SEM photographs of the samples synthesized by solid state reaction with various revealed particles $Pb_{7.6}Eu_{0.4}Na_2(PO_4)_6\square_{0.8}O_{0.2}$ (a and b), $Pb_8Na_2(PO_4)_6\square_{(2-x/2)}$ (c and d).

Table 1

Results of the SEM of $Pb_{(8-x)}Eu_xNa_2(PO_4)_6\square_{(2-x/2)}$ for x=0.0 and x=0.4, which synthesized by solid state reaction

x	P		Pb		Eu		Na		O	
	Calcd	found	Calcd	found	Calcd	found	Calcd	found	Calcd	found
0	8.18	8.86	72.80	74.84	-	-	2.02	1.51	16.9	15.21
0.4	8.24	8.72	69.84	69.59	2.69	2.54	2.03	1.42	17.17	16.74

As initial data for the refinement of the crystal structure using the coordinates of the atoms in the structure of calcium hydroxyapatite, which are presented in [17, p. 10], as well the results of the work [18, p. 10], which showed that the sodium ions in two

predominantly the structure $Pb_8Na_2(PO_4)_6$ localized in position Pb(1). Refinement was carried out for compositions *x*=0 and 0.8 for 851 and 907 reflections and 34 parameters and 33, respectively. Reliability factors for *x*=0.0 and x=0.8: 8.13 and 5.68 (Rp); 10.5 and 7.15 (Rwp); 6.48 and 5.79 (Rf); 6.51and 6.03 (Rb); 1.56 and 1.69 (χ^2), respectively.

Previously it was shown that the replacement of the structure of calcium hydroxyapatite the predominantly cationic positions determined by the difference of the effective charges of ions replace each other. In that case if the effective charge of the substitute ion is smaller than the ion Ca^{2+}, it take the place of Ca(1), if more - Ca(2) [19, p. 10]. A similar pattern is observed upon substitution of the lead by europium in the solid solutions structure $Pb_{(8-x)}Eu_xNa_2(PO_4)_6\square_{(2-x/2)}O_{(x/2)}$. Since the effective charge of Pb^{2+} ions is less than the effective charge of ions Eu^{3+}, then the last substitution in the apatite structure of Pb^{2+} ions are located in positions Pb(2) structure is presented in Table 2 and 3.

Table 2

Crystallographic data and atomic coordinates of $Pb_{7.2}Eu_{0.8}Na_2(PO_4)_6\square_{0.6}O_{0.4}$ sample obtained by solid state reaction from Rietveld analysis

Space group: P63/m (VOL. A, 176) Unit cell parameters: a =9. 73074 (Å); c = 7. 17399 (Å); v =588.279 (Å^3)						
Atom	Site	Site Occupancy	x	y	z	Beq (Å^2)
Pb1	4f	1.491(50)	2/3	1/3	-0.00181(335)	1.239(162)
Na1	4f	2.000	2/3	1/3	-0.00181(335)	1.239(162)
Eu1	4f	0.509(50)	2/3	1/3	-0.00181(335)	1.239(162)
Pb2	6h	5.709(50)	0.25456(54)	0.99628(85)	1/4	1.128(84)
Eu2	6h	0.291(50)	0.25456(54)	0.99628(85)	1/4	1.128(84)
Na2	6h	-	0.25456(54)	0.99628(85)	1/4	1.128(84)
P	6h	6.000	0.40550(237)	0.37854(219)	1/4	0.451(448)
O1	6h	6.000	0.44449(500)	0.56545(628)	1/4	5.083(793)
O2	6h	6.000	0.66653(502)	0.49304(552)	0.08083(364)	5.083(793)
O3	12i	12.000	0.35079(308)	0.25664(366)	1/4	5.083(793)
O4	4e	0.400	0	0		

Table 2 showed the atomic parameters, Site Occupancy and Equivalent Isotropic Thermal Displacement Parameters for $Pb_{7.6}Eu_{0.4}Na_2(PO_4)_6\square_{0.6}O_{0.4}$, moreover Table 3 showed the occupancy of Pb(1) and Pb(2) in the structures $Pb_8Na_2(PO_4)_6$ and $Pb_{7.2}Eu_{0.8}Na_2(PO_4)_6\square_{0.6}O_{0.4}$.

As a result, refinement of the crystal structure was calculated interatomic distances; some of them are showed in Table 3. As can be seen from Table 3 the localization of europium ion in the position of Pb(2) structure causes a decrease in the average distances Pb(2)-O(1,2,3), that due to the lower crystal ionic radius of Eu^{3+} in comparison with ionic radius of Pb^{2+} [16, p. 10], but ion Eu^{3+} has a large charge in comparison with the charge

of ion Pb^{2+}. Decrease in the interatomic distances in the polyhedron Pb(2) in turn causes an increase in the interatomic distances in the polyhedron Pb(1).

Table 3

Selected Interatomic Distances $Pb_{(8-x)}Na_2Eu_x(PO_4)_6\square_{(2-x/2)}O_{(x/2)}$ for Varying Values of *x*

	x = 0	*x* = 0.8
Pb(1)–O(1) x 3	2.35(3)	2.55(4)
Pb(1)–O(2) x 3	2.59(3)	2.40(4)
Pb(1)–O(3) x 3	2.81(3)	2.85(4)
< Pb(1)–O >	2.58	2.60
Pb(2)–O(1)	2.63(4)	2.52(7)
Pb(2)–O(2)	2.29(4)	2.19(4)
Pb(2)–O(3) x 2	2.43(2)	2.53(4)
Pb(2)–O(3) x 2	2.77(3)	2.54(3)
< Pb(2) – O(1-3) >	2.55	2.475
Pb(2) – O(4)	-	2.496(7)
< Pb(2)–O >	-	2.486
P–O(1)	1.65(5)	1.42 (6)
P–O(2)	2.21(5)	1.81 (5)
P–O(3) x 2	1.59 (3)	1.68(3)
< P–O >	1.76	1.65
Pb(2) – Pb(2)	4.349(8)	4.323(9)

The infrared absorption spectra of $Pb_{(8-x)}Eu_xNa_2(PO_4)_6\square_{(2-x/2)}O_{(x/2)}$ with x=0.0, 0.2, 0.4 and 0.6 show characteristic absorption bands of the phosphate groups $(PO_4)^{3-}$ and H_2O of the apatitic structure. All bands are shown in infrared spectrum Fig. 5.

The two strong lines (x=0.0), located at 987 and 1050 cm^{-1}, and assigned to the triply-degenerate asymmetric stretching (ν3) mode of phosphate, appearing at high wavenumbers than $Pb_{10}(PO_4)_6F_2$ (1041 and 980 cm^{-1}) and $Pb_{10}(PO_4)_6(OH)_2$ (1041 and 985 cm^{-1}) [21, p. 10], but approximate to $Pb_8Na_2(PO_4)_6$(1056 and 990 cm^{-1}) [22, p. 10,11].

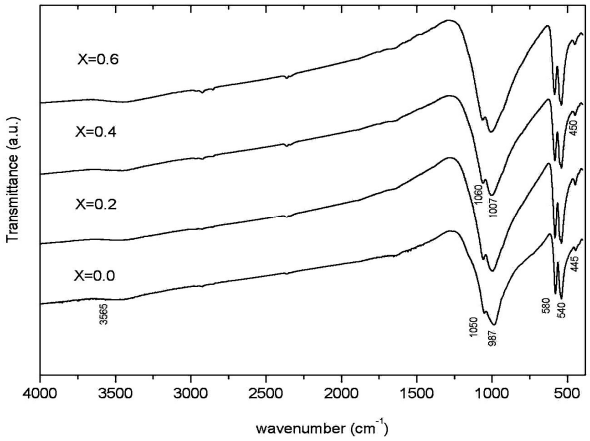

Fig. 5. Infrared spectra of $Pb_{(8-x)}Na_2Eu_x(PO_4)_6\square_{(2-x/2)}O_{(x/2)}$ solid solutions with x=0.0, 0.2, 0.4, 0.6.

CONCLUSIONS

1. Experimental syntheses, FTIR, XRD, and SEM investigations of PbAP were reported, focusing upon a composition $Pb_{(8-x)}Eu_xNa_2(PO_4)_6\square_{(2-x/2)}O_{(x/2)}$. The site of the atoms in the solid solutions was also analyzed by the Rietveld method. The grain sizes ranged from several dozen to several hundred nanometers. It was established, that the limit of the isomorphism substitution in the composition $Pb_{(8-x)}Eu_xNa_2(PO_4)_6\square_{(2-x/2)}O_{(x/2)}$ corresponds with the value x <1.2. The results of lattice parameters showed, that the unit cells *a* and *c* and were decreased, when the value x is increasing..
2. The infrared spectrum showed, a shifting of the internal vibration modes of the $(PO_4)^{3-}$ toward higher wavenumber as the lead contents decreases. Refinement of the crystal structure showed that the europium ions are mainly occupied in the sites of Pb(2) the structure of apatite, resulting in mean interatomic distances Pb(1)-O(1,2,3) increases, while the P-O decreases. This unexpected fact demonstrates that the changes in interatomic distances are controlled not only by the geometrical factor, the difference in sizes of the ions involved in the substitution, but also by their charges as well. This finding has practical importance for choosing new substituents and enhancing adsorptive, catalytic, and other important properties of apatite.

References

1. Rakovan J. Structural Characterization of U(VI) in Apatite by X-ray Absorption Spectroscopy / J. Rakovan, R.J. Reeder, E.J. Elzinga et al. // Environ. Sci. Technol. – 2002. – V. 36. – P. 3114–3117.
2. Manecki M. Uptake of aqueous Pb by Cl–, F–, and OH– apatites: Mineralogic evidence for nucleation mechanisms / M. Manecki, P.A. Maurice, S.J. Traina // Am. Miner. – 2000. – V. 85. – P. 932–942.
3. Laperche V. Effect of Apatite Amendments on Plant Uptake of Lead from Contaminated Soil / V. Laperche, T.J. Logan, P. addam, S.J. Traina // Environ. Sci. Technol. – 1997. – V. 31. – P. 2745–2753.
4. Yamashita K. Humidity-sensitivity of yttrium substituted apatite ceramics / K. Yamashita, H. Owada, T. Kanazawa et al. // Solid State Ionics. – 1990. – V. 35. – P. 401–404.
5. Blasse G. Influence of local charge compensation on site occupation and luminescence of apatites / G. Blasse // J. Solid State Chem. – 1975. – V.14. – P. 181–184.
6. Gaft M. Luminescence of Pr3+ in minerals / M. Gaft, R. Reisfeld, G. Panczer, E. Uspensky, B. Varrel, G. Boulon // Optical Materials . – 1999. – V. 13, № 1. – P. 71–79.
7. Cantelar E. Optical characterisation of rare earths in natural fluorapatite / E. Cantelar, G. Lifante, T. Caldero´n et al. // Journal of Alloys and Compounds – 2001. – V.323-324 – P. 851–54.
8. Serret A. Stabilization of calcium oxyapatites with lanthanum (III) – created anionic vacancies / A. Serret, M.V. Cabanas, M. Vallet-Regi // Chem. Mater. – 2000. – 12. – P. 3836–3841.
9. Get'man E. Isomorphous substitution of europium for strontium in the structure of synthetic hydroxovanadate / E. Get'man, N. Yablochkova, S. Loboda et al. // J. Solid. State Chem. – 2008. –V. 181. – P. 2386–2392.
10. Ardanovaa L. Isomorphous Substitutions of Rare Earth Elements for Calcium in Synthetic Hydroxyapatites / L. Ardanovaa, E. Get'man, S. Loboda et al. // Inorg. Chem. – 2010. – V. 49. – P.10687–10693.
11. Verbeeck R. Lattice parameters and cation distribution of solid solutions of calcium and lead hydroxyapatite / R. Verbeeck, C. Lassuyt, H. Heijligers, F. riessens // J. Calcif. Tissue Int. – 1981. – V. 33. – P. 243–247.
12. Brixner L. Optical and electronic properties of some new rare earth-doped lead sodium apatites / L. Brixner and P. Bierstedt // J. Solid State Chem. – 1975. – V. 13. – P. 24–31.
13. Rodriguez_Carvajal J. Program FullProf.2k (version 3.40. November 2005. LLB JRC) (unpublished).

14. Roisnel T., Rodriguez_Carvajal J. WinPLOTR: a Windows tool for powder diffraction patterns analysis / T. Roisnel, C.-J. Rodriguez // Mat. Sci. Forum. Proc. of the Seventh Europ. Powder Diffraction Conf. (EPDIC 7). Barcelona – 2000. – P. 118.
15. Mayer I. Lead phosphate apatites substituted by rare earth, sodium, and potassium ions / I. Mayer, A. Semadja and V. Weiss / I. Mayer // Journal of Solid State Chemistry.– 1980.– V. 34.– P 223–229.
16. R. D. Shannon R. D. Revised effective ionic radii in halides and chalcogenides / R. D. Shannon // Acta Crystallogr. A. – 1979. – V. 32. – P. 751–767.
17. Wilson R. Rietveld refinement of the crystallographic structure of human dental enamel apatites / Wilson R; Elliot J; Dowker S. / R. Wilson // American Mineralogist. – 1999. – V.84. – P. 1406–1414.
18. El Koumiri M. Crystal structure of the lacunar apatite NaPb4(PO4)3 / M. El Koumiri , S. Oishi, S. Sato et al. // Materials Research Bulletin. – 2000. – V. 35. – P. 503–513.
19. Cantelar E. Optical characterisation of Rare Earths in natural apatite / E. Cantelar, G. Lifante, T. Caldero´n et al. // Journal of Alloys and Compounds. – 2001.– P. 323–24.
20. Laghzizil A. Comparison of Electrical Properties between Fluoroapatite and Hydroxyapatite Materials / A. Laghzizil, N. El Herch, A. Bouhaouss, G. Lorente and J. Macquete // J. Solid State Chem., 2001.– V. 156.– P 57–60.
21. Toumi M. Crystal structure and spectroscopic studies of Na2Pb8(PO4)6 / M. Toumi, T. Mhiri// Journal of the ceramic society of Japan.– 2008.– V. 116(8).– P 904–908.
22. Andres-Verges M. On the structure of calcium-lead phosphate apatites / M. Andres-Verges, F. J. Higes-Rolando, C. Valenzuela-Calahorro and P. F. Gonzalez-Diaz // Spectrochimica Acta Part A: Molecular Spectroscopy.– 1983.– V. 39.– P. 1077–1082.

Гетьман Е.И. Исследование кристаллической структуры композиции $Pb_{8-x}Eu_xNa_2(PO_4)_6\square_{2-x/2}O_{x/2}$ / Е.И. Гетьман, А.В. Игнатов, Мухаммед А.Б. Абдуль Джабар, С.Н. Лобода // Ученые записки Таврического национального университета им. В.И. Вернадского. Серия «Биология, химия». – 2011. – Т. 24 (63), № 3. – С.48-56

Методом рентгенофазового анализа изучено замещение ионов свинца ионам европия в соединении $Pb_8Na_2(PO_4)_6\square_2$ в соответствии со схемой $Pb^{2+} + ½\square \rightarrow Eu^{3+} + ½O^{2-}$, что соответствует образованию твердых растворов состава $Pb_{8-x}Eu_xNa_2(PO_4)_6\square_{2-x/2}O_{x/2}$ ($0 \le x \le 2,0$). Найдено, что замещение при температуре 800 °С, происходит в области составов до $x < 1,0$. Уточнение кристаллической структуры некоторых образцов проведено с помощью метода Ритвельда. Установлено, что ионы празеодима локализуются преимущественно в позиции Pb(2). Показано, что параметры ячеек практически не изменяются, в то время как средние межатомные расстояния Pb(1) – O(1,2,3) заметно возрастают, а P – O – уменьшаются.

Ключевые слова: структура апатита, твердые растворы, свинец, европий.

Гетьман Є.І. Дослідження кристалічної структури композиції $Pb_{8-x}Eu_xNa_2(PO_4)_6\square_{2-x/2}O_{x/2}$ / Є.І. Гетьман, О.В. Ігнатов, Мухамед А.Б. Абдуль Джабар, С.М. Лобода // Вчені записки Таврійського національного університету ім.В.І. Вернадського. Серія „Біологія, хімія”. – 2011. – Т. 24 (63), № 3. – С. 48-56.

Методом рентгенофазового аналізу досліджено заміщення іонів плюмбуму іонами європію в сполуці $Pb_8Na_2(PO_4)_6\square_2$ у відповідності зі схемою $Pb^{2+} + ½\square \rightarrow Eu^{3+} + ½O^{2-}$, що відповідає утворенню твердих розчинів складу $Pb_{8-x}Eu_xNa_2(PO_4)_6\square_{2-x/2}O_{x/2}$ ($0 \le x \le 2,0$). Знайдено, що однофазні тверді розчини, за температури 800°С, утворюються в області до $x < 1,0$. Уточнення кристалічної структури деяких зразків проведено з використанням алгоритму Рітвельда. Встановлено, що іони Празеодиму переважно локалізуються в позиції Pb(2). Показано, що параметри комірок практично не змінюються, у той час як середні міжатомні відстані Pb(1) – O(1,2,3) помітно зменшуються, а P – O – збільшуються.

Ключові слова: структура апатиту, тверді розчини, плюмбум, європій.

Поступила в редакцию 10.09.2011 г.